

Ages of asteroid families with the YORP-eye method

Paolo Paolicchi,^{1*} F. Spoto,² Z. Knežević³ and A. Milani⁴

¹*Dept. Physics, University of Pisa, Largo Pontecorvo 3, I-56127 Pisa, Italy*

²*IMMCE, Observatoire de Paris, Av. Denfert-Rochereau 77, 75014 Paris, France*

³*Serbian Academy of Sciences and Arts, Kneza Mihaila 35, 11000 Belgrade, Serbia*

⁴*Dept. Mathematics, University of Pisa, Largo Pontecorvo 5, I-56127 Pisa, Italy*

Accepted XXX. Received YYY; in original form ZZZ

ABSTRACT

We have recently shown the possibility of finding footprints of the YORP effect concerning the members of asteroid dynamical families, in a plot proper semimajor axis–magnitude (the so-called “V–plot”), and in spite of several biases and uncertainties. That work introduced the concept of the “**YORP–eye**”, the depopulated regions in the plot above, whose location is diagnostic of the age of the family.

In the present paper we complete the analysis using an improved algorithm and an extended database of families, and we discuss the potential errors due to uncertainties and dispersion of the astronomical data. We confirm that the analysis connected to the search for the YORP-eye can lead to an estimate of the age, which is similar and strongly correlated to that obtained by the analysis of the V–slope size dependent spreading due to the Yarkovsky effect.

In principle the YORP-eye analysis alone can lead to an estimate of the ages of other families, which have no independent age estimates. However, these estimates are usually affected by large uncertainties and, often, not unique. Thus they require a case–by–case analysis to be accepted, even as a rough first estimate.

Key words: Asteroids – Asteroids, rotation – YORP effect – dynamical families – age of families

1 INTRODUCTION

In a recent paper (Paolicchi and Knežević 2016), hereinafter referred to as “Paper I”, the possibility of detecting footprints of the YORP effect in asteroid dynamical families by analyzing the distribution of its members in the so-called V–plot (absolute magnitude H or inverse size $1/D$ vs. proper semimajor axis a) has been extensively discussed. As it is well known, the YORP effect often causes the migration of the spin vector pole towards extreme obliquities measured from the normal to the orbital plane (Vokrouhlický and Čapek 2002; Bottke et al. 2002, 2006; Micheli and Paolicchi 2008; Nesvorný and Vokrouhlický 2008; Vokrouhlický et al. 2015). In dynamical families, this process has to be combined with the migration in semimajor axis due to the diurnal Yarkovsky effect (Farinella et al. 1998; Farinella and Vokrouhlický 1999; Bottke et al. 2002; Chesley et al. 2003; Vokrouhlický et al. 2015), which is faster (for a given size of the body) for extremely oblique rotation axes. The clustering of axes causes a clustering in a close to the borders of the V–plot of several families (Vokrouhlický et al. 2006; Bottke et al. 2015). However, this

effect is not easily detected for other families (Spoto et al. 2015).

In Paper I we introduced the so-called “central depletion parameter” $R(H)$ as function of the absolute magnitude, and discussed how the maxima of $R(H)$ can provide information about the age of the family. We assumed that a maximum depletion is present at a given H whenever the duration of a YORP cycle, for that value of H , is equal (or proportional, with a fixed constant of proportionality) to the age of the family. This assumption led to the definition of the “**YORP–eye**”. In Paper I we introduced an adimensional parameter “YORP-age” (represented in the equations as Y_{age} , see eq. 6), which, assuming $f(A) = 1$ (see Paper I for a discussion), is simply given by the equation:

$$Y_{age} = \tau_f A / a^2 \quad (1)$$

where τ_f is the age of the family (in My), A the albedo and a the semimajor axis (in au).

If we know the age and the other average properties of the family we are able to compute Y_{age} and, in turn, to estimate at what value of H the maximum of the function $R(H)$ is expected. The main purpose of Paper I has been the comparison between the expected and computed maxima,

* E-mail: paolo.paolicchi@unipi.it

and the main result has been that they are often not too different, and fairly well correlated.

In this paper the analysis attempted in paper I is improved, extended and carried to more quantitative and detailed conclusions. The analysis is extended to 48 families for which [Milani et al. \(2016, 2017\)](#) estimated the age. The estimate was based on the spreading of the V-plot with time, as a consequence of the Yarkovsky effect. These families are hereinafter referred to “Yarkaged families”). This sample is larger compared to that used in Paper I, due both to an increased list of Yarkaged families and to the possibility, allowed by the new version of the algorithm, of performing a reliable analysis of smaller families (down to 100 members, compared to the 250 members in the previous work). As in Paper I, we performed this analysis on the basis of the $a-H$ V-shaped plots of the various families, using a sample of about 130000 family members, classified according to the method discussed in [Milani et al. \(2014\)](#), within a general list exceeding 500000 objects. We enclose in our list also a few families, again with a number of members exceeding the minimum value, for which no previous age estimate exists (hereinafter “un-Yarkaged families”).

2 NEW DATA, NEW ALGORITHM AND AN IMPROVED ANALYSIS.

In the present paper we analyzed a total of 64 families with more than 100 members, obtained from the current version of the “Astdys” database. By means of the method discussed in [Milani et al. \(2014\)](#), for 36 of them, a twofold age estimate has been provided, computed from the slope of left (or “IN”) and right (or “OUT”) wings of the V-plot; usually, the two values are not exactly equal, even being in a few cases significantly different. However, for 33 families it has been possible to reconcile the two estimates, which are consistent within an error bar ([Milani et al. 2017](#)). For the remaining 3 families the two ages are definitely inconsistent with each other. These families may have a peculiar collisional history; the two ages may correspond to different events. For instance, in the case of the family of (4) Vesta the fragments have presumably been created by two (or more) cratering collisions. For 12 “one-sided” families only one age estimate has been possible; again, it may be a consequence of a complex collisional history and also of dynamical processes: the family may be asymmetrical due to the cutting effect of a strong resonance. The analysis of individual cases has been presented in separate papers. Finally, the remaining 16 families have no age estimate obtained with the method based on the Yarkovsky effect (“un-Yarkaged families”), even if, for some of them, other age estimates are available in the literature. The main properties of the families in our sample have been detailed in Tables 1, 2 and 3.

The analysis of the updated set of families has been improved with a small but relevant change in the algorithm. In paper I we searched for the maxima of the depletion parameter $R(H)$ with a running box method, with a fixed *boxsize* of 100 bodies. The choice was conservative, excluding the possibility of analyzing small families, and also potentially masking significant features especially in the low- H tail, where a jump by 100 bodies may mean to pass in a single step from the largest bodies to by far smaller ones. The main purpose

Table 1. Summary of the data for the families used in the computations. The present table lists those with two consistent estimates of *Yarkage*. For each family (Corfam= label of the core family - see [Spoto et al. \(2015\)](#)) we first list the number of members (Mem). We then give the average value of the the geometrical albedo (AveAl), and its dispersion in the family (Alvar). Next we give the average proper semimajor axis of the family (in *au*). Finally we present the age (in *My*) computed according to [Milani et al. \(2014\)](#) method (age) and the estimated error (ager). The updated estimate of the error is computed according to the method discussed in [Milani et al. \(2017\)](#). Note also that the family 163 is the combination of the nominal family 163 with the family 5026, that we list as family 293 that whose largest member is in reality the asteroid 1521, as family 110 that whose largest member is the asteroid 363 (Padua), as family 194 that whose largest member is the asteroid 686 (Gersuind). Note also that the family 18405 was already named as Brixia (521 Brixia is now considered a background object) and that we take the “nominal” family 31, in spite of the problems discussed in the text. For what concerns the family 9506, see the discussion in the Subsection 4.7.

Corfam	Mem	AveAl	Alvar	sma	age	ager
3 Juno	1693	0.253	0.060	2.670	463	110
5 Astraea	6169	0.269	0.080	2.580	328	71
10 Hygiea	3147	0.073	0.020	3.160	1347	220
20 Massalia	7820	0.249	0.070	2.400	180	27
24 Themis	5612	0.069	0.020	3.150	3024	632
31 Euphrosyne	1384	0.061	0.020	3.150	1225	304
110 Lydia	899	0.171	0.040	2.740	238	40
158 Koronis	7390	0.240	0.060	2.890	1746	296
163 Erigone	1023	0.055	0.010	2.370	224	36
194 Prokne	379	0.150	0.040	2.590	1448	348
221 Eos	16040	0.157	0.050	3.040	1466	216
293 Brasilia	845	0.174	0.040	2.850	143	56
302 Clarissa	236	0.053	0.020	2.400	50	10
396 Aeolia	529	0.106	0.030	2.740	95	21
434 Hungaria	1869	0.380	0.100	1.940	206	45
480 Hansa	1164	0.286	0.070	2.630	895	164
569 Misa	647	0.058	0.020	2.650	259	95
606 Brangane	325	0.121	0.030	2.580	46	8
668 Dora	1742	0.058	0.010	2.780	506	116
808 Merxia	1263	0.248	0.060	2.750	329	50
845 Naema	375	0.065	0.010	2.940	156	23
847 Agnia	3336	0.242	0.060	2.780	753	151
1040 Klumpkea	1815	0.204	0.100	3.130	663	154
1128 Astrid	548	0.052	0.010	2.780	150	23
1303 Luthera	232	0.052	0.010	3.220	276	62
1547 Nele	344	0.355	0.070	2.640	14	4
1726 Hoffmeister	2095	0.048	0.010	2.780	332	67
1911 Schubart	531	0.039	0.010	3.970	1557	343
3330 Gantrisch	1240	0.047	0.010	3.150	460	128
3815 Konig	578	0.051	0.010	2.570	51	10
9506 Telramund	325	0.245	0.070	2.990	219	49
10955 Harig	918	0.251	0.070	2.700	462	121
18405 1993FY12	159	0.184	0.040	2.850	83	21

of Paper I, however, was to show that the YORP-eye search is a sensible and useful concept, and that the results can provide hints about the age of the family. From this point of view, such a conservative and cautious approach was reasonable.

In the present paper we are instead interested in obtaining significant information about the age and in comparing it with other family age data, but also in introducing the possibility of using the YORP-eye method alone to get a first

Table 2. The same as in Table 1 but for the families with two ages which cannot be explained with a single collisional event (first three lines) and for families with only one age estimate. A zero value is given when the age estimate has not been possible. The data “age1” and “age1er” refer to the left or “IN” wing, while “age2” and “age2er” refer to the right or OUT wing. Note also that we list as family (93) Minerva that for which in reality the largest member is the asteroid 1272 Gefion.

Corfam	Mem	AveAl	Alvar	sma	age1	age1er	age2	age2er
4 Vesta	10612	0.355	0.10	2.36	930	217	1906	659
15 Eunomia	9756	0.260	0.08	2.62	1955	421	1144	236
25 Phocaea	1248	0.253	0.120	2.32	1187	319	0	0
87 Sylvia	191	0.059	0.020	3.52	0	0	1119	282
93 Minerva	2428	0.256	0.100	2.77	1103	386	0	0
135 Hertha	15984	0.060	0.020	2.39	761	242	0	0
145 Adeona	2069	0.062	0.010	2.65	794	184	0	0
170 Maria	2958	0.261	0.080	2.59	0	0	1932	422
283 Emma	577	0.049	0.01	3.05	290	67	628	234
375 Ursula	731	0.062	0.020	3.17	3483	1035	0	0
752 Sulamitis	193	0.055	0.010	2.44	341	109	0	0
945 Barcelona	346	0.300	0.100	2.62	203	56	0	0
1658 Innes	775	0.264	0.070	2.58	0	0	464	143
2076 Levin	1536	0.202	0.070	2.29	0	0	366	125
3827 Zdenekhorsky	1050	0.074	0.020	2.73	154	34	0	0

Table 3. The same as in Table 1 and in Table 2 but for the un–Yarkaged families.

Corfam	Mem	AveAl	Alvar	sma
96 Aegle	120	0.071	0.010	3.06
148 Gallia	137	0.268	0.070	2.76
298 Baptistina	177	0.210	0.070	2.27
410 Chloris	120	0.095	0.030	2.74
490 Veritas	2139	0.070	0.020	3.17
778 Theobalda	574	0.066	0.020	3.18
883 Matteredania	170	0.274	0.100	2.24
1118 Hanskyia	116	0.057	0.010	3.20
1222 Tina	107	0.160	0.030	2.79
1298 Nocturna	186	0.073	0.030	3.15
1338 Duponta	133	0.279	0.100	2.28
2782 Leonidas	111	0.065	0.010	2.68
12739 1992DY7	298	0.186	0.100	2.72
13314 1998RH71	241	0.051	0.010	2.78
18466 1995SU37	257	0.240	0.080	2.78
31811 1999NA41	144	0.126	0.040	3.11

guess for the age independently from the other results possibly present in the literature. In order to improve our potential of analysis we have systematically reduced the box size. According to Paolicchi et al. (2017), who analyzed several different sizes, the reduction of the *boxsize* does not affect significantly the results, with the exception of some features occurring in the distribution tail containing the large bodies. In the present paper we used the *boxsize* of 20 bodies for families of up to 250 members, of 30 in the range 250 – 2000 and of 50 for the largest families. Moreover, in a few cases, we have explored the limit case with *boxsize* = 10. As we will discuss in the following, this choice is sometimes appropriate to improve the resolution of the $R(H)$ function, and sometimes necessary to inspect the features close to the $low - H$ region.

In the present paper we have also introduced a further improvement, in order to avoid the occurrence of meaningless “unphysical” maxima. While the large members of a family are usually well below the observational complete-

ness limit, and thus they are fully representative of the mass/size distribution within the family (apart the presence of potential interlopers, not always easily identified), the *high - H* tail is severely biased. In general we expect a distribution dn/dH monotonically increasing with H , at least within a significant range. Thus a decrease is diagnostic of observational selection effects (maybe combined with evolutionary effects (Morbidelli et al. 2003)). In our analysis we have truncated our search of maxima of $R(H)$ at H values for which the distribution dn/dH has already significantly begun to decrease. Typically the resulting cut-off is at $H = 16/17mag$ which is, by the way, usually not critical for our search of the YORP-eye. We will analyze this point in detail in the following.

We wish here to discuss another significant aspect, concerning the resulting plots of the depletion parameter.

The plots we used previously (Paolicchi and Knežević 2016) were showing only the maxima of the function $R(H)$: i.e. we have kept only the values $RMAX(H)$ which are local maxima. However, the maxima are often very numerous, and also the function $RMAX(H)$ exhibits in some cases sawtooth-like features or high-frequency fluctuations. Thus we have identified the “significant maxima” looking at the plot of $RMAX(H)$ and searching for “maxima of the maxima”. When several significant maxima are present within a small H range we select only the one with the highest value of R . In this way we have selected a number N_{max} of significant maxima which is usually 2 (the most frequent case) or 3, with a few cases with only one maximum and one case for which $N_{max} = 4$.

From the point of view of the theory, we know that:

- The original properties of the family may (or may not) entail one – or even more than one – maximum R which is usually masked by the subsequent evolution, but which can survive if it involves the large bodies (whose orbital elements are not affected – or are only moderately affected – by the Yarkovsky driven mobility).

- We have no idea, at the moment, of what happens after several YORP-cycles. Maybe the central depletion is partially or totally masked –this has been our starting assumption

tion when searching for the YORP-eye – but it is also possible that other significantly depleted regions appear.

- Due to the above arguments, the YORP-eye due to YORP/Yarkovsky effects should correspond to significant maximum of R located at the smallest or at the second smallest value of H (exceptionally, to the third one – see below the discussion concerning the family of (221) Eos). We have systematically followed this guideline, to choose among multiple significant maxima.

- We have no way to distinguish theoretically between the “candidate” maxima, as defined above, thus, whenever possible, we have chosen one providing a better fit with the Yarkovsky estimated age. The physical processes affecting the original properties and the evolution of the V-plot with time are extremely complex. Among the others, the presence of resonances can open gaps which can mix with those due to YORP effect, or even mask them. Thus, being able to detect footprints, also in such a fuzzy context, is a significant success.

- In some cases the possible maxima do not suggest any reasonable agreement (also taking into account the errors) with the Yarkovsky ages. As we will discuss in the following, these cases (which we will call “OUTRANGE”) can be easily explained in terms of an elementary statistical argument. In other cases we have only one-wing Yarkovsky age definition, or two values which are strongly different. A discussion case-by-case is required. Finally we have families without any previous age estimate. We can use the values obtained from the YORP-eye method but, unfortunately, we have to keep all the estimates based on the various candidate maxima.

The problem of multiple maxima is explained also by the Figure 1.

3 “GOOD” AND “BAD” CASES

For several families the analysis of $RMAX(H)$ and the comparison of the significant maxima to the values expected according to the available age estimates is straightforward. In these cases the two ages estimated by the slope of the two wings in the V-plot, according to Yarkovsky effect, are nearly equal. Among the 36 families with two age estimates, in 33 cases the two values can be considered as consistent, and a best fit value, together with an error bar, can be computed. If the most significant maximum of the depletion parameter is sharp and close to the value(s) expected according to the estimated ages, we are in a definitely “good” case, as it happens, for instance, for the Family of (845) Naema. In Figure 2, top panel, we represent the $RMAX(H)$ function, compared to the expected values, while we enclose also, for comparison, the V-plot of the same family (Figure 2, bottom panel). Note that here and in the following R-plots we compare the $RMAX(H)$ function with the maxima which are expected from the Yarkovsky-driven slope of the V-plot, not taking into account the possible offset due to the calibration (see also the discussion in paper I). However, we can anticipate that, as a result of the present improved and extended computations, the offset will be rather small, with relevant consequences only for the age estimate of very young families. In fact, as we will discuss in the next Section, the age computed according to YORP-eye method, and with the standard calibration (defined in Paper I) has to be decreased

by less than 20%. This calibration entails a change in the relevant H by about 0.15 mag, a small correction not affecting the present discussion. However, the best-fit analysis reveals the presence of an additional constant term in the calibration, of the order of $50My$, which can be relevant for the young families.

The case of family (221) Eos is a little more troublesome. The $RMAX(H)$ plot (Figure 3, top panel) exhibits two very sharp maxima around $mag = 11$: one of them is even above the upper limit of the figure. However, as it is easy to see from Figure 3 (bottom panel), in the corresponding magnitude region the family is extremely asymmetric, and these maxima are presumably dependent on the original properties of the family itself. Thus, in this only, very peculiar case, the third (in order of increasing H) significant maximum can be taken into account. Note that it provides a very good fit with the expected values. However, as can be seen by inspection of Figure 3 (bottom panel), the original properties of the family play a role also for this feature.

Different problems concern the dynamical families with two inconsistent age estimates. These two estimates may be related to a complex collisional history. For instance, the two different slopes of the wings of (4) Vesta family may be correlated with the two past major collisional events, witnessed by the two big craters featuring on the surface of the asteroid (Rheasilvia and Veneneia). Thus every family is, in principle, a unique case, and we can expect different outcomes also from our YORP-based analysis. For instance for the family of (283) Emma the comparison of $RMAX(H)$ with the two expected maxima shows a potentially significant maximum (unfortunately not very sharp) close to the “OUT” expected values, as shown in Figure 4. Note that, as discussed in Paper I, also maxima for which $R < 1$ can be significant. For what concerns the “IN” expected maximum we can find a rather poor fit with the absolute maximum of $RMAX(H)$ or a very good fit with another weakly significant maximum. In these cases the comparison is less significant, entailing arbitrary choices.

The problem of asymmetric families, especially those for which only one wing provides an estimate of the age, is very complex. The causes of the asymmetry are different and not always unequivocal. We have discussed in Paolicchi et al. (2017) a few cases for which the asymmetry is mainly due to the presence of neighboring resonances. In these cases a possible improvement of the analysis can be achieved by a “mirroring” procedure. However, since the improvements are not always very significant, and since the uncritical extension of the mirroring procedure to all the asymmetric families would be wrong, we have used for our analysis, in the case of single-aged family, the nominal family and the available age as the benchmark for comparison.

Finally, we have several cases for which it is difficult to obtain an acceptable fit between the YORP and Yarkovsky ages, even taking into account the errors. For most cases the reason is simple: the expected maxima are in the range of H for which we do not have enough bodies for a sensible statistical analysis. Often, but not always, the involved families are old, thus the expected YORP eye is in a region with very few large bodies. In several cases it is possible to solve the problem, and find a significant maximum, repeating the computation with a reduced $boxsize = 10$ value. The resulting $RMAX(H)$ curve is obviously more noisy. Note also

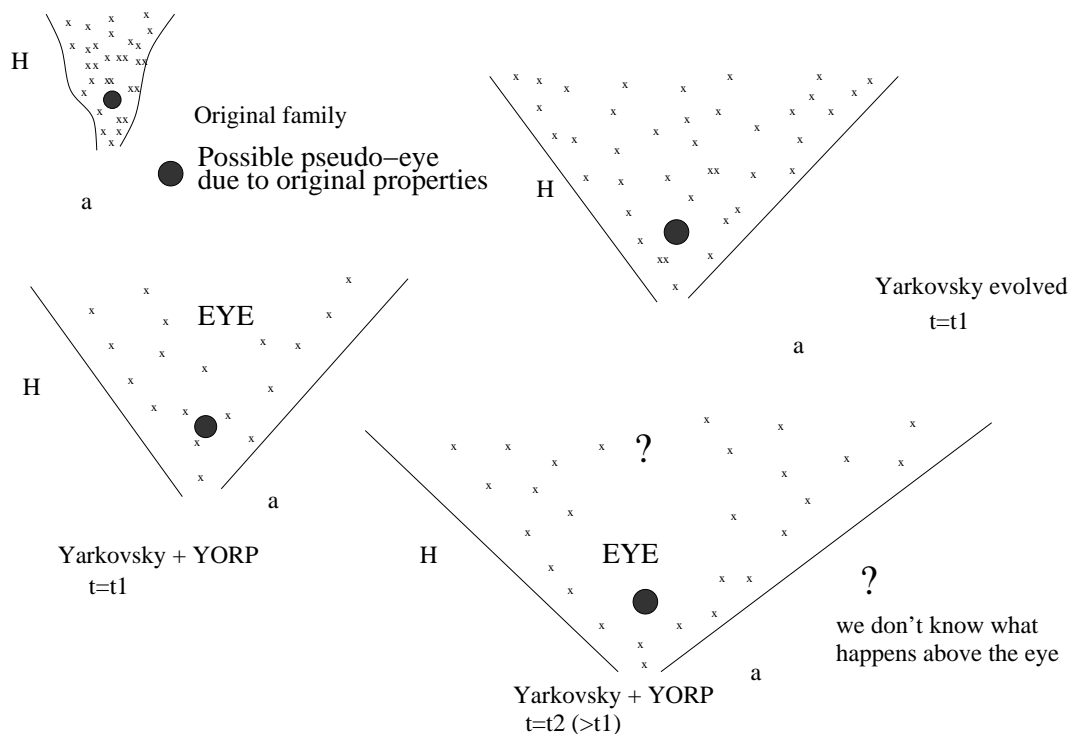


Figure 1. The figure schematically represents the expected appearance of the regions in the $a - H$ plane occupied by the members of a family (a is in abscissa, H in ordinate). The top left figure refers to the initial structure of the family, as originated in the family-forming collision, and due to the individual properties of the colliding bodies, to the impact geometry, and so on: the shape is not clearly defined, even if a slight general trend towards a larger spread in a for the smaller members can be expected. In this plot a “false YORP-eye” (dark circle) can appear, due to the original distribution of orbital elements. If this false eye is in the region of large objects, which evolve slower, it can be preserved also at later times. The other figures represent the evolved family, taking into account Yarkovsky and YORP effects, with the expected formation of the true YORP-eye, and the uncertainties concerning what happens at later times, after several YORP cycles. We recall that the eye shifts with time towards the region of brighter objects.

that the value of $RMAX$ computed with a reduced $boxsize$ is usually larger. The explanation is trivial: the range in a , which is used to define the seven a bins (see Paper I for a detailed discussion) in the box corresponding to a given value of H , is fixed by the extreme a values in the box. With this definition, the extreme bins (1 and 7) gain both one body from scratch. This bias is negligible for large values of $boxsize$, not so when we have a total of 10 bodies in the box.

The case of the family of (163) Erigone (combined, as in Paper I, with the family of (5026) Martes) is representative of those which can be solved with a reduced $boxsize$. As shown by Figure 5, it is possible to find a maximum very close to the expected values only with the choice of a reduced $boxsize$. With the normal $boxsize$ the expected values are simply out of the domain of the function $RMAX(H)$.

For other families it is simply impossible, even reducing the value of the $boxsize$, to obtain maximum values of the function for H corresponding to the expected values. For the reasons which will become more clear in the following, we have “discarded” the cases for which not only we do not find a good fit of Yarkovsky/YORP ages, but also because taking as significant maximum the lowest H value in the $RMAX(H)$ we obtain a YORP-age lower than half the Yarkovsky one. Note that the “factor 2 in age” criterion (see the discussion below) corresponds essentially to a difference of about 0.75 mag in the magnitudes between the expected

and the computed maxima. The criterion to reject the fit is more severe than those used in Paper I; consequently the number of “OUTRANGE” families is larger.

The list of these “OUTRANGE” families is reported in Table 4.

The problems concerning the identification of a good fit for several families can be clarified by Figure 6.

As shown by the figure, for all the “OUTRANGE” cases the number of bodies is extremely low (sometimes even 0 or 1), thus the search of a significant maximum in the relevant H range cannot be performed even with a reduced $boxsize$. The cases for which the fit has been performed with the reduced $boxsize$ correspond to rather low numbers of bodies in the region of the expected maximum. We have the only exception of the family 1726 for which we adopted a reduced $boxsize$ to obtain a more detailed $RMAX(H)$, even if the expected maximum is in the range for which we have more than 100 brighter objects. Note that also the nominal $RMAX(H)$ might lead to a reasonable fit.

In conclusion the main reason for failure or difficulties to find the fit is essentially statistical (too few members in the relevant H , or size, range). Similar problems might arise looking for a fit within very young families, where the relevant H range is in a region where we have no bodies or the number of bodies is severely diminished by observational selection effects. Fortunately, the only very young family with a “Yarkage” is that of (1547) Nele, which is bright enough

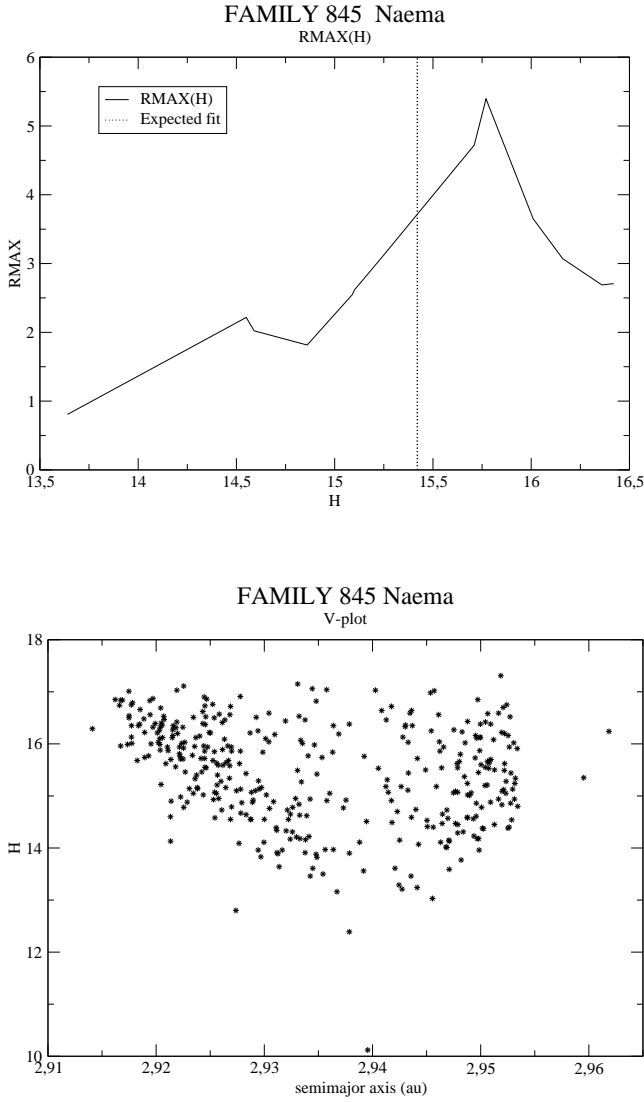


Figure 2. Top panel: the figure represents the $RMAX(H)$ function for Family 845, compared to the expected value, which is in a fair agreement with the computed maximum. Bottom panel: V-plot of the Family 845. The central depletion is apparent, even if the identification of the maximum depletion at $H \simeq 16$ mag is not that obvious.

and located in the inner part of the Main Belt, thus allowing to find a significant number of bodies with high enough H (around $mag = 16$).

4 RESULTS AND DISCUSSION

4.1 The Yarkovsky-YORP comparison: uncertainties and errors

The present analysis allowed us to identify, for the families with a previous age estimate, the significant maxima of $RMAX(H)$ and, consequently, to obtain a new estimate of the age based on the YORP effect. However, the prob-

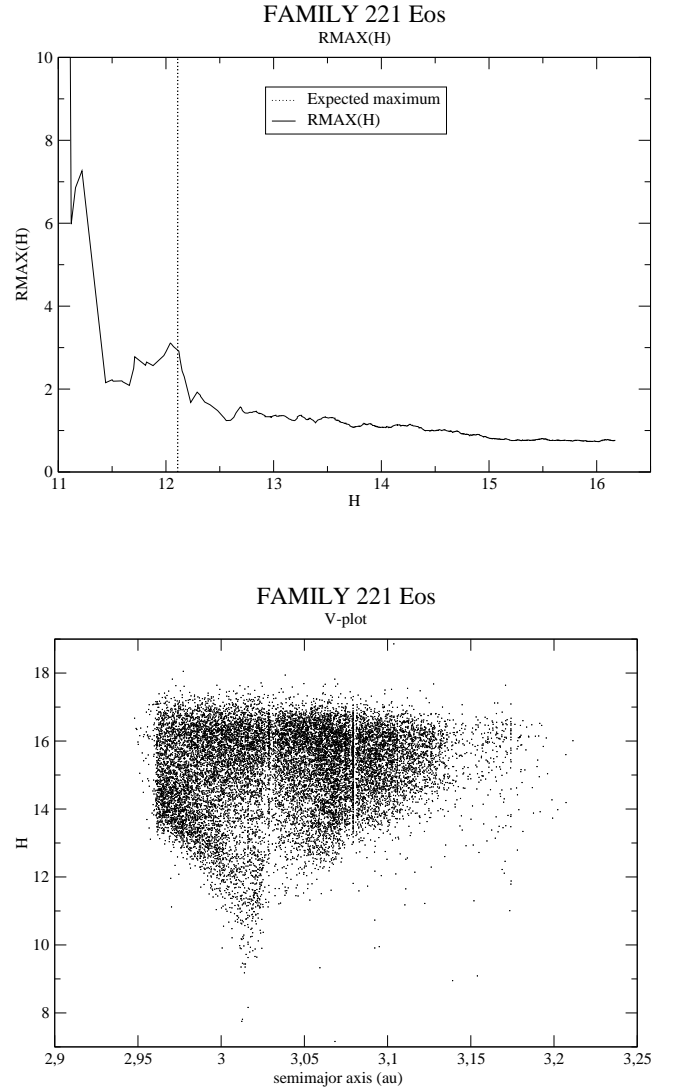


Figure 3. Top panel: the figure represents the $RMAX(H)$ function for Family (221), compared to the expected value, which is in good agreement with the obtained significant maximum, however, not the one corresponding to the highest value. Bottom panel: The figure represents the V-plot of the Family (221). The left-right asymmetry seems to dominate the overall structure of the family at least for what concerns the bright objects.

lem of calibration discussed in Paper I remains unsolved, thus the age is defined up to a multiplicative constant. A complete and updated model, including YORP, Yarkovsky, collisions and, in some cases, other dynamical mechanisms connected –for instance– to resonances, does not exist, thus we are bound to refer to the first pioneering attempts by [Vokrouhlický et al. \(2006\)](#). However, we can at least offer a couple of considerations:

- In principle, after one YORP cycle, the spin of the bodies should be preferentially oriented close to the normal to the orbit plane, thus maximizing the effectiveness of the Yarkovsky drift. However, since the spin clustering may be

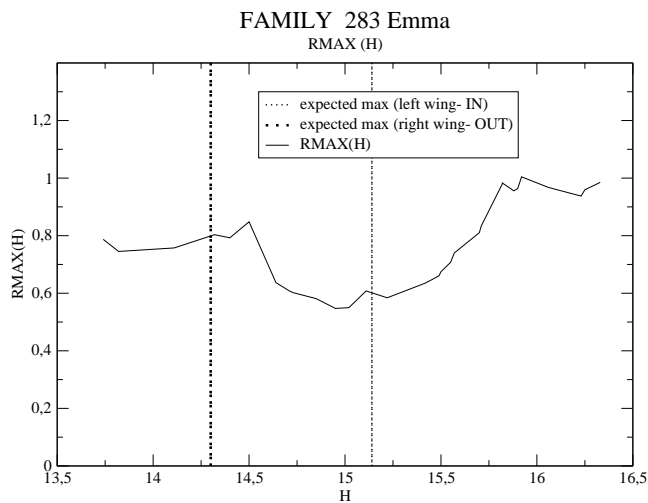


Figure 4. The figure represents the $RMAX(H)$ function for Family (283), compared to the expected values (left and right wing); they are very different, but both not far from local maxima of the curve.

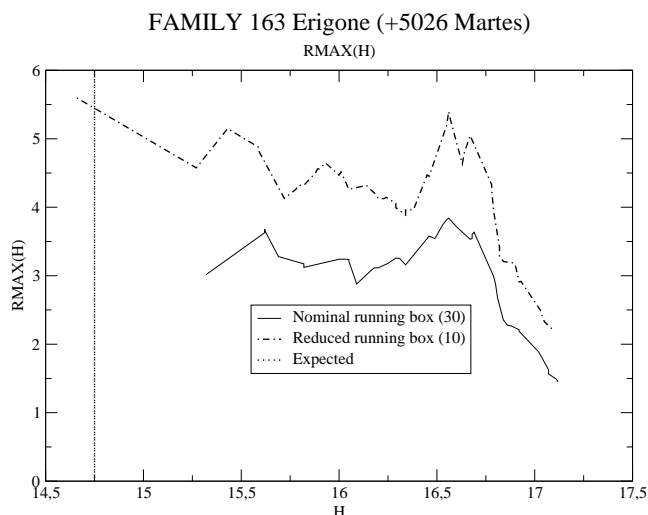


Figure 5. The figure represents the $RMAX(H)$ function for Family 163, compared to the expected values (left and right wing); $RMAX$ is computed also with a reduced $boxsize$.

partially or totally disrupted by collisions, maybe the maximum clustering will be reached before this time; it is also possible, due to a complex combination of effects, that the maximum clustering will be reached at a later time. This uncertainty has to be added to the basic uncertainty due to the calibration of the YORP effect itself, which may also depend on additional parameters, such as size – apart from the well known $1/D^2$ dependence – or taxonomy, or porosity, or else. Essentially, we have no *a-priori* indication whether the age at which a maximum R at a particular value of H (the “eye”) occurs is larger or smaller than the duration of the YORP cycle corresponding to the same H . The results we are going to discuss might, in principle, provide a hint concerning this point, but the combination of several uncertainties, the partial subjectivity of our choice of significant maxima, and the intrinsically unknown parameters do not allow to consider them enough accurate.

Table 4. The “OUTRANGE” families (see text). For these families the “Yarkage” (in My) obtained with the analysis based on the Yarkovsky effect significantly exceeds the maximum age (“max Yage”) which would be obtained by the YORP method were the significant maximum located exactly at the *low* – H edge. We recall that family 194 is now currently defined as (686) Gersuind. Note that the family 4 has been reported twice, using the two inconsistent *Yarkages*. Note also that the family (1658) Innes exhibits a severe asymmetry due to dynamical reasons, and might be corrected with the mirroring procedure described in Paolicchi et al. (2017).

Corfam	Yarkage	minimum H	max Yage
3 Juno	463	14.11	110
4 Vesta	930	13.03	171
4 Vesta	1906	13.03	171
20 Massalia	180	14.84	46
194 Prokne	1448	14.01	195
434 Hungaria	206	14.31	33
480 Hansa	895	12.83	310
1658 Innes	464	13.67	97
2076 Levin	366	13.77	140
10955 Harig	462	14.76	63

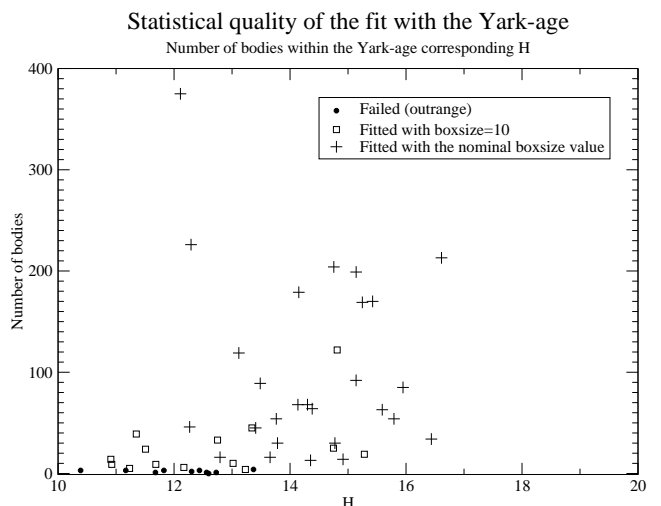


Figure 6. The figure represents the number of bodies brighter than the H value corresponding to the expected maximum of $RMAX(H)$, according to the estimated Yarkovsky ages (nominal values). The families for which the fit has been impossible are represented as filled circles; those for which the fit has been done with a reduced $boxsize$ are represented with squares, while those for which the fit has been performed with the nominal $boxsize$ are represented by crosses.

- Defining the *Ansatz* in Paper I we have ignored that the formation of the “eye” requires both the spin clustering and a significant Yarkovsky drift after this clustering. It may introduce an additive offset term in the calibration. We expect that, given the different dependence of YORP and Yarkovsky effects on the size (respectively $\propto 1/D^2$ and $\propto 1/D$), this term is more important for small objects, thus for younger families.

It is also worth discussing the errors of the age estimates, and the possible definition of an error bar. The errors involved in the estimate of the age obtained from the

Yarkovsky effect (generally not small) have been estimated in Milani et al. (2017). For most families the nominal value of the age and of the respective error have been obtained as a sort of a weighted average between the “IN” and “OUT” estimated ages. The error bars will be represented by the horizontal bars in Figure 8. Error bars will be available also for the (3) cases in which the “IN” and “OUT” estimates cannot be reconciled, and we remain with a double age. It is possible that these two ages correspond to two collisional events, as it appears to have happened in the above mentioned case of the family of (4) Vesta. In a way, these cases are not too different from the more numerous cases for which only one wing has been used to obtain an estimate of the age. These families have presumably often underwent complex post-collision evolutionary paths, involving i.e. resonances. Also in this case an error bar is available. However, since we have used for the final calibration only the families with two consistent *Yarkages*, we decided not to represent the corresponding error bars of these two last groups in the Figure 8.

For what concerns the error in the definition of the age estimated from YORP effect, in this case we have essentially two terms. One, due to the above discussed calibration and similar problems, is essentially unpredictable, and has been ignored in our estimates; the other, easier to handle, is connected to the uncertainties/dispersion of the albedo and of the semimajor axis. Let us consider the definition of YORP-age given in Paper I and recalled by 1.(eq. 6). Then if we have a distribution of A with average A_{mean} and standard deviation ΔA (often rather large), and a distribution of a with average a_{mean} and standard deviation Δa , we obtain:

$$\frac{\Delta Y_{age}}{Y_{age}} \simeq \frac{\Delta A}{A_{mean}} + 2 \frac{\Delta a}{a_{mean}} + \Delta \tau_f / \tau_f \quad (2)$$

where $\Delta \tau_f$ refers to the uncertainty of the age estimate, which can be obtained from the literature. In principle this argument may lead to estimate the uncertainty of the expected value of maximum $R(H)$, and thus to decide whether the expected and the computed maxima are consistent each other. However, there are two reasons to follow a different path: the errors in albedo and age are usually large, thus the linear approach in Eq.2 is less reliable. Moreover, and more important, we are willing to extend our consideration also to families for which a previous age estimate does not exist. Thus we start from the computed maximum of $R(H)$ to define an age estimate, which we will call in the following *Yorpage*, to be compared, whenever possible, to the existing age estimates. The uncertainty $\Delta Y_{orpage}/Y_{orpage}$ is due only to the spreads in albedo and semimajor axis, and is then given by the equation:

$$\frac{\Delta Y_{orpage}}{Y_{orpage}} \simeq \frac{\Delta A}{A_{mean}} + 2 \frac{\Delta a}{a_{mean}} \quad (3)$$

The estimates of the error range between 20% and 50% (see also Table 5); the related error bars are represented (vertical bars) in Figure 8, for the same families for which we have given the *Yarkage* error bars. Obviously the same uncertainty applies to the actual age estimates obtained by the YORP effect.

4.2 Yorpage vs Yarkage plots

Before passing to the final comparison, which will include a calibration, we can introduce a raw plot, comparing the ages for different groups of objects.

Note that we will discuss a few peculiar cases in the following. At this stage we are using all the nominal data as they are.

The relevant groups we are going to analyze are the following:

- All families: we include in this sample all the families with any *Yarkage* estimate, excluding those which have been identified as “OUTRANGE”; those with two consistent ages are included twice; it does not affect the figure, but is relevant for the computation of linear regression (see below).
- Families with a “good” *Yarkage*: the subset of the previous one including only those with two consistent *Yarkages*.
- A recent paper (Milani et al. 2018) explicitly divides the families between “fragmentation” and “cratering”; we define a sample with only the cratering families. Note that, for the purpose of the present work, we are not taking into account the possible problems connected with this classification, i.e. transition or ambiguous cases.
- As above, we define a sample with only the fragmentation families.

In Figure 7 we represent these four samples in a single plot. We have plotted the age obtained with the YORP analysis (hereinafter *Yorpage*, to be distinguished from the definition of Y_{age} used above and in Paper I) vs. the age estimated on the basis of the Yarkovsky effect (*Yarkage*). Obviously the symbols referred to the fragmentation and cratering families are superimposed to those corresponding to “all” and “good” samples. Also for cratering or fragmentation samples, the objects with two consistent ages are reported twice. In the figures we represent also the linear regression plots referred to the samples. As it is easy to see, they indicate in all cases a small negative offset (a few tens of My) and a coefficient of proportionality α which is typically moderately larger than unity. Indeed the proximity of α to the unity is a good and significant news, not at all predictable. Also the offset may have a physical significance. As we have discussed in the previous Subsection, our “Ansatz” (the *Yorpage* is equal to the duration of a YORP cycle for the magnitude where the maximum of $R_{MAX}(H)$ appears) was neglecting the time required by Yarkovsky effect to move the objects in semimajor axis. This neglected time is more relevant for the smaller objects, due to the different size-dependence of YORP and Yarkovsky effect; thus the young families (for which the relevant maximum corresponds to small objects) may seem “younger” when their age is computed with the YORP method. Note, however, that the estimated offset resulting from the regression relation may be a dominant effect for very young families; for these objects the calibration, which we will discuss below, may overcorrect the estimated age (see the discussion in the following). The coefficients referred to “all” and “good” samples amount to about 1.2, that corresponding to fragmentation families is slightly smaller, while it becomes steeper for cratering families. There is no obvious explanation for this difference, and we have to remark that the cratering families are few, thus the difference might be due to statistical fluctu-

ations. However, further analysis may be useful, also with the perspective of a fraction of cratering families increasing in the future (Milani et al. 2018).

Finally we are going to introduce in the plot the error bars and the calibration issue.

We have made a choice which we consider as reasonable: since the families with only one Yarkovsky age, and those with two inconsistent ages are expected to have undergone a complex collisional (multiple relevant collisions) or dynamical (truncating resonances, and so on) evolution, we decided to consider for the final calibration only those (27) with two ages, i.e. those defined as “good”. The calibration thus consists in dividing the YORP computed age by a factor $\alpha = 1.2471$ and adding a constant offset of $55.35 My = 69 My/\alpha$. The calibrated *Yorpages* are plotted against the *Yarkages* in Figure 8. In the figure we include also the error bars corresponding to the uncertainty in the *Yarkage* (horizontal bars) and to the internal error of the *Yorpage* (vertical bars). We represent also the families with one (or two inconsistent) ages, without error bars, with the same calibration. As it is obvious, the regression line of the “good” families has angular coefficient equal to unity, and no offset; with the same calibration, as can be expected according to the results previously discussed, the regression for all families has an angular coefficient slightly smaller than unity (about 0.92) and a moderate positive offset. We decided not to represent the error bars of these additional families (which are, typically, of similar size to the others), to keep a good readability of the graph.

For what concerns the quality of the fit, we see that, at least for the “good” families, the error bars cross the fit line in most cases. There are a few exceptions, however.

Taking into account that the typical YORP and Yarkovsky errors are of a few tenths, that they are at least in part independent from each other, and that the 2σ acceptance level is reasonable, we have decided to consider the result good enough whenever the Yarkovsky and YORP estimates are within a factor 2. We have only three cases exceeding this limit. We will improve the analysis in the following, when introducing the total error estimate. The analysis will show that we are even conservative taking these three cases as “troublesome”. One of these three cases is that of family 1726, whose anomalous behaviour may be connected to the peculiar shape properties discussed by Novaković (2015). The other two cases refer to two rather young families, i.e. 1547 and 3815; in these two cases the obvious explanation is connected to the constant offset term in the calibration, which dominates the final age estimates for these young families (see also the discussion below).

The results are not seriously affected by these poorly fitted families. In order to verify this statement we have tried to eliminate all the families not within the above mentioned factor 2 in age. The results are plotted in Figure 9.

The overall fit is not significantly altered; the regression line for the “good” families has now a coefficient of about 1.01, and that for all families remains essentially the same; only the constant offset terms are a little different; consequently our results are sufficiently robust and reliable.

In Table 5 we represent the overall properties of the “good” families, relevant for the plot represented in Figure 8. We have also introduced an estimate of the total standard error *toterr*, for a more precise evaluation of the qual-

ity of the fit between *Yorpage* and *Yarkage*. It is a rough estimate, since we are not analyzing the possible interdependences of the errors, and other possible problems. Essentially we assume that:

$$toterr = \sqrt{\left(\frac{\Delta Yarkage}{Yarkage}\right)^2 + \left(\frac{\Delta Yorpage}{Yorpage}\right)^2} \quad (4)$$

where, obviously, ΔX is the error related to the quantity X .

We enclose in the table also several ‘quality codes’, which answer simple, but relevant questions:

- Is the adopted maximum one that corresponds to the absolute maximum of $RMAX(H)$? YES=0 NO=1.
- Does the adopted maximum $RMAX$ exceed unity? YES=0 NO=1.
- Is the adopted maximum within 1σ (=0) or 2σ (=1) with respect to the *Yorpage* (NO=2)? Note that we have computed the standard error multiplying the larger between *Yarkage* and *Yorpage* with the relative total error. This procedure leads to obtain a fit below 2σ for all the families, except 1547. It may be a little optimistic, but not unreasonable. Note that as *Yorpage* we have used the calibrated value.
- Has the adopted maximum been obtained with a reduced *boxsize*? YES=1 NO=0.
- Are there significant maxima at smaller values of H , compared to the adopted one: NO=1, one significant maximum =2, two significant maxima =3. According to the discussion in the previous Section of what we do understand theoretically, the maxima corresponding to the lowest or to the second lowest H value are usually the most significant.

Finally note that in the case of family 302, the location of the YORP-eye in a is almost exactly coincident with a relevant resonance. It is the most striking case (but not the only one) of interferences between the features due to the physical evolution and those due to dynamical processes. In this case the observed “eye” is partially or totally due to the resonance, and the claimed “good” result might even be an artifact. In other cases the interference may be disruptive. We have kept this family in our list, since the purpose of the paper is essentially of statistical nature. However, we warn again the reader that if results concerning individual cases are looked for, they require a thorough and detailed analysis case per case.

4.3 Particular cases: families 31,87,569,9506

The results presented in the previous Subsection are statistical; the families are analyzed with a general algorithm, ignoring their peculiarities. Even if the overall results, which are of a statistical nature, are robust and do not depend on these peculiarities, it is worth discussing some particular cases, to which Milani et al. (2018) devoted a detailed discussion. The families we are going to consider are of (31) Euphrosyne, (87) Sylvia, (569) Misa and (179) Klytaemnestra (or, as discussed below, of (9506) Telramund).

4.4 (31) Euphrosyne

According to the discussion presented in the above quoted paper, this dynamical family has a very complex struc-

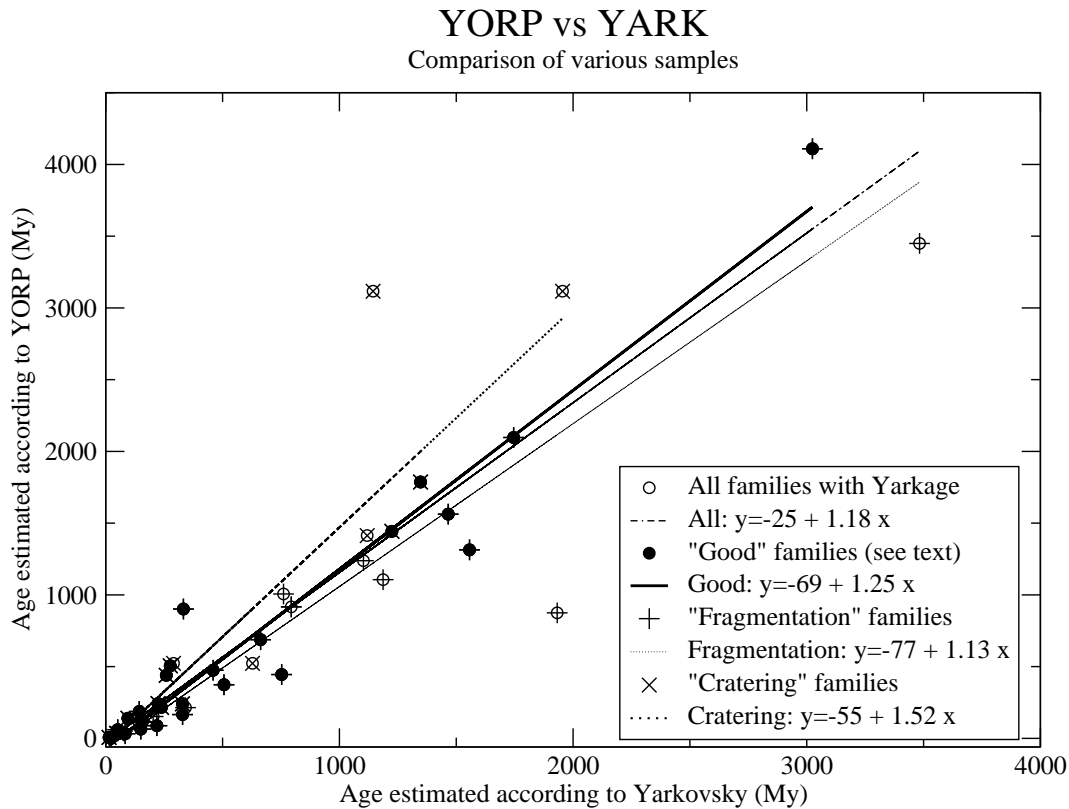


Figure 7. The figure shows the uncalibrated Yarkovsky and YORP ages for the samples described in the text. Linear regression plots are added. The symbols are explained in the figure legend.

ture, and might even be formed by three collisional families, one corresponding to the wings used for the *Yarkage* estimate, and two others, probably much younger and compact. We are not going to analyze this or alternative possibilities, nor the overall role of the resonant regions, studied by Machuca and Carruba (2012). Our purpose is only to discuss why our age estimate (performed with the use of the complete family, including all bodies) is in a very good agreement with the *Yarkage*.

In Figure 10 we plot, in the V-plot of the family, a line corresponding to the H value for which we have identified the relevant $RMAX$. As it is possible to see from the figure, at this level the dominant role of the resonant region, discussed by Milani et al. (2018), is not yet completely effective, and the structure seems to exhibit a wider empty region (unfortunately the statistics is rather poor, since large bodies are involved). Thus it is not surprising that we have found a maximum with a very good fit with that expected for the complete family, because precisely the large bodies shape the wings which are significant to compute the *Yarkage*.

4.5 (87) Sylvia

The case of family of (87) Sylvia is not completely different. Also in this case the structure of the V-plot is dominated by a resonant region. Also in this case, the potentially significant $RMAX$ is at a low H value, for which we have few bodies, all on one side of the resonance; thus it is not possible identify possible YORP footprints not making part of

the empty region caused by the resonance. The Figure 11 shows this controversial case.

4.6 (569) Misa

According to Milani et al. (2018) the family of (569) Misa contains another subfamily, that of 15124, 2000 EZ39. The separation of the two families is rather difficult, since the largest remnants of both families have a very similar semi-major axis. However, it is possible to define the family 15124, with about 500 members, and obtain an estimate of the age, slightly above $100My$. We have not included the family 15124 in the statistical analysis discussed above, but we have run our code and obtained $RMAX(H)$. The main maximum of the function corresponds, after calibration, to an age of about $200My$, with a reasonable agreement with the *Yarkage*, taking into account all the uncertainties concerning the identification of the family. The V plot of the family is reported in Figure 12, together with a line referred to the maximum of $RMAX$.

4.7 (9506) Telramund

According to the discussion in Milani et al. (2018) the family of (179) Klytaemnestra may be an artifact of the clustering method. In reality, the real and relevant family should be a subset, for which the leading body is (9506) Telramund. In the present paper we have taken for granted this analysis, and used the family 9506 as the significant one.

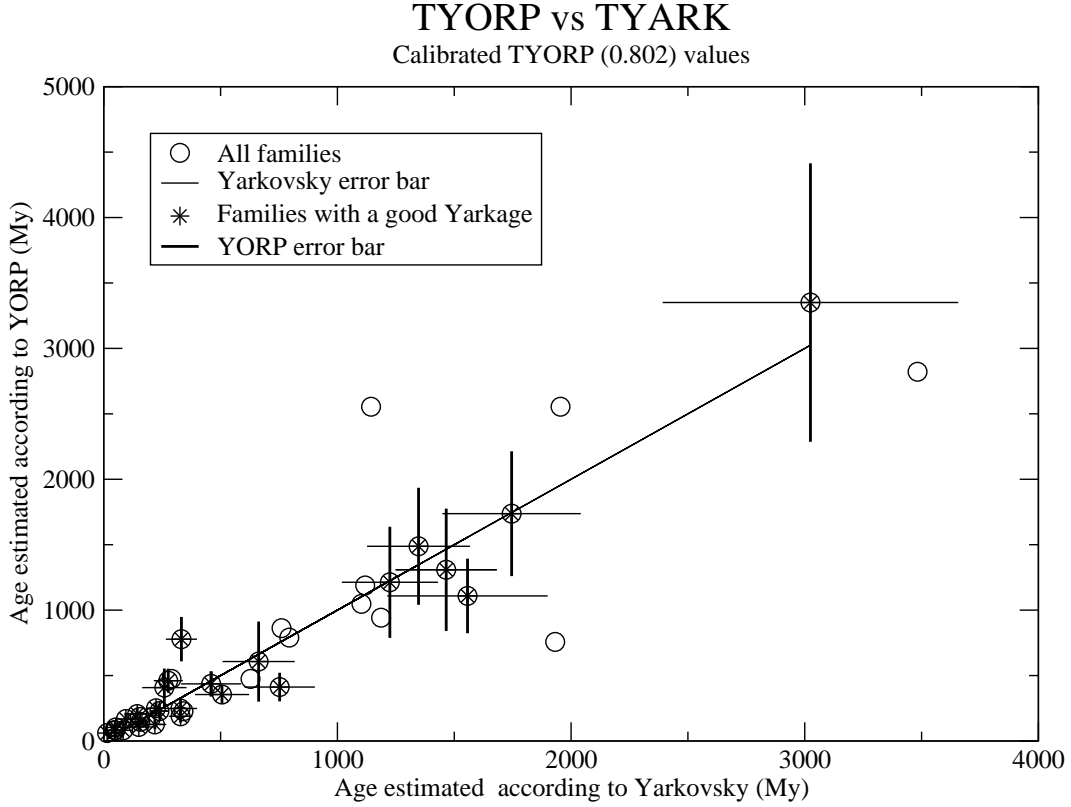


Figure 8. The plot represent the families after the calibration of the *Yorpage*. In abscissa the *Yarkage* is plotted. In ordinate we represent the calibrated *Yorpage* (see text). The line corresponds to the best linear fit, including also a constant offset. The horizontal error bars refer to the estimated error bar for *Yarkage*, while the vertical error bars refer to the *Yorpage* uncertainty due to the dispersion of albedo and semimajor axis within the family.

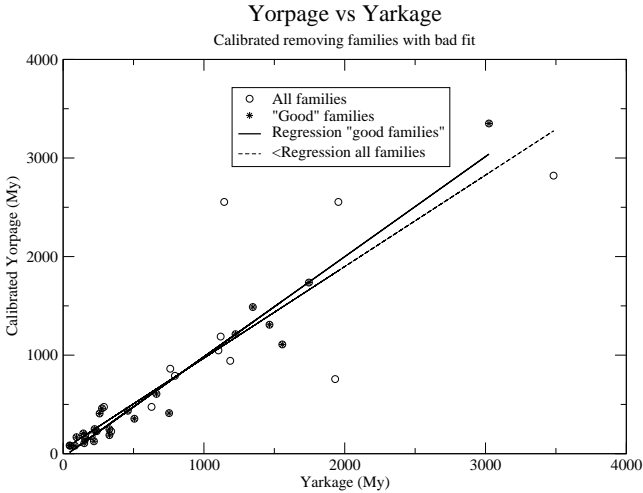


Figure 9. The plot represents the families without those for which the calibrated *Yorpage* and the *Yarkage* were different by more than a factor 2; we adopted the same normalization as in the previous figure. We represent also new regression lines.

4.8 The “un-Yarkaged” families

The 16 families listed in Table 3 do not have any age estimate based on the Yarkovsky method. We have included them in our computations, obtaining for each of them a $RMAX(H)$ function. We used the same approach as for other families to

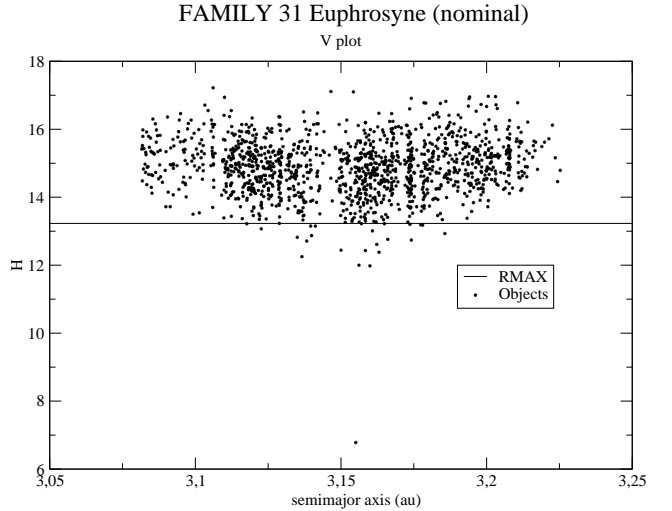


Figure 10. In the V plot of family of (31) Euphrosyne we represent, with a horizontal line, the H value at which we find the significant maximum of $RMAX(H)$ which we adopted to estimate the *Yorpage*.

detect the significant maxima. However, in the present case, we have no independent indication, thus we have no criterion for a choice among them. Thus, we obtain a list of potential ages computed according to the YORP-based method; the list is slightly subjective, but reliable in principle, since

Table 5. The table represents a synthetic summary of the results for the “good” families. We recall the recent changed identifiers for families 293 (now 1521) and 110 (now 363). For every family we report the *Yarkage*; the calibrated *Yorpage*, the estimated error for *Yorpage*; the total estimated error (see text); five quality codes (absolute maximum, value of maximum, difference compared to σ , boxsize reduction code, order of adopted maximum starting from low H ; see text for details); in some cases notes are present: 1= see text.

corfam	<i>Yarkage</i>	<i>Yorpage</i>	erryorp	toterr	absmax	valR	sig	box	order	notes
5 Astraea	329	248	0.31	0.38	0	0	0	0	1	
10 Hygiea	1347	1488	0.30	0.34	1	1	0	0	1	
24 Themis	3024	3350	0.32	0.38	1	0	0	0	1	
31 Euphrosyne	1225	1213	0.35	0.39	0	1	1	1	1	1
110 Lydia	238	229	0.25	0.30	1	1	0	0	1	
158 Koronis	1746	1737	0.28	0.32	1	0	0	1	1	
163 Erigone	224	250	0.20	0.26	0	0	0	1	1	
221 Eos	1466	1308	0.36	0.39	1	0	0	0	3	1
293 Brasilia	230	283	0.24	0.46	1	1	0	0	1	
302 Clarissa	50	81	0.38	0.44	1	0	0	0	1	
396 Aeolia	96	48	0.29	0.36	0	0	1	1	1	
569 Misa	259	408	0.36	0.51	1	0	0	0	1	1
606 Brangane	46	83	0.25	0.30	0	0	1	0	1	
668 Dora	506	355	0.18	0.29	0	0	1	0	2	
808 Merxia	329	188	0.26	0.30	1	0	1	1	1	
845 Naema	156	147	0.16	0.34	0	0	0	0	1	
847 Agnia	753	412	0.27	0.33	0	0	1	1	1	
1040 Klumpkea	663	607	0.50	0.55	1	0	0	1	1	
1128 Astrid	150	107	0.20	0.25	0	0	0	0	1	
1303 Luthera	276	461	0.20	0.30	1	0	1	0	2	
1547 Nele	14	61	0.20	0.35	1	1	2	0	2	
1726 Hoffmeister	332	778	0.22	0.30	0	0	1	1	1	
1911 Schubart	1557	1109	0.26	0.34	1	1	0	0	2	
3330 Gantrisch	460	436	0.22	0.35	0	0	0	0	1	
3815 Konig	51	104	0.20	0.28	1	0	1	0	2	
9506 Telramund	219	126	0.29	0.37	1	1	1	0	1	1
18405 1993FY12	83	81	0.22	0.28	0	0	0	0	1	

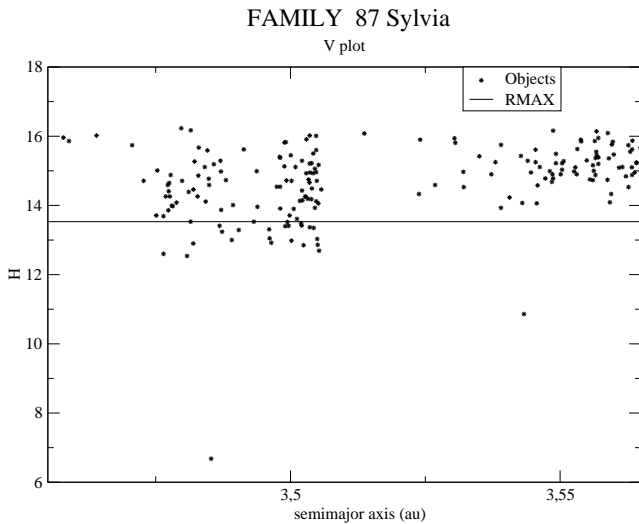


Figure 11. In the V plot of family of (87) Sylvia we represent, with a horizontal line, the H value at which we find the significant maximum of $RMAX(H)$ which can be adopted to estimate the *Yorpage*.

we have used the same method which has given good results for the other families. Unfortunately, we have no way to discriminate among the multiple maxima, whenever they are present, and our outcome is only a list of possible ages, with the hope to be able to confirm or falsify them with

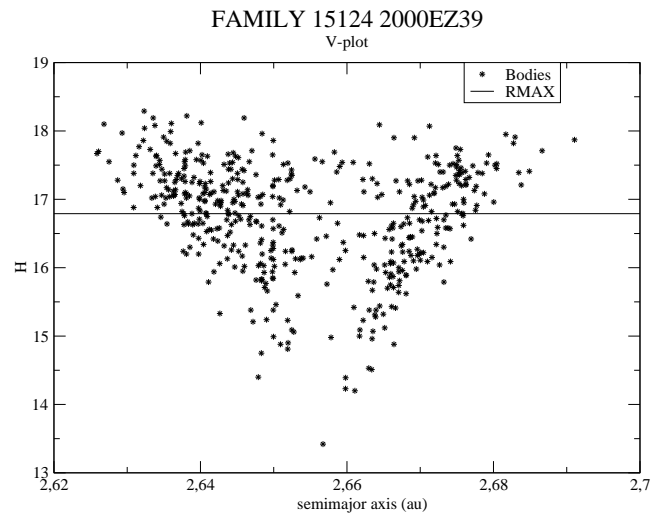


Figure 12. In the V plot of family 15124 we represent, with a horizontal line, the H value at which we find the significant maximum of $RMAX(H)$ which we adopted to estimate the *Yorpage*.

a forthcoming analysis, case per case, based also on additional information. The goal of the present paper is limited to obtaining this list. Anyway, we are prepared for a comparison with the Yarkovsky based ages, which will be available in the future, or which can be guessed somehow also from the data already available, even with a worse precision than usual. It is thus worth converting the computed *Yorpage*

to what could be expected, were the *Yarkage* obtainable. In the previous discussion we have found a correction factor and a fixed offset required to obtain, on the average, coincident YORP and Yarkovsky ages. The overall equation is of the form:

$$Yorpage = A + B Yarkage \quad (5)$$

where A and B are constant quantities. Thus:

$$Yarkage = Yorpage/B - A/B = Corr_{Yage} + 55.35 \quad (6)$$

where the quantities are, as usual, in *My*. $Corr_{Yage}$ is the corrected (by a factor $A = 0.802$) value of the age used to obtain the plot in Figure 8.

Moreover, we have a few weak indications from the Yarkovsky based analysis, and a pair of age estimates obtained with different methods: (490) Veritas (Knežević et al. 2006; Carruba et al. 2018), and (778) Theobalda (Novaković 2010). Thus we are going to give a list of potential ages, with a synthetic conclusion, and a few notes about the possibility of accepting these estimates as reliable.

The list of these families and of their suggested ages is presented in Table 6.

Notes:

- According to the above quoted estimates present in the literature, the families 490 and 778 are very young, thus the suggestions presented in the Table have to be considered not meaningful.
- Five families of the sample have $Mem \leq 120$ (see Table 3). These families do not have any *Yarkage* since the number of their members is too low to allow a significant statistical analysis; probably the same considerations apply also to our *Yorpage* estimates. Since future updates of the database and thus the growth of family memberships are expected we decided to hold these cases for future reference.
- For the other families, age estimates may be available in the next future. By the way, while preparing the present draft, a new Yarkovsky based age determination has been added (for family 87; see Table 2). The estimated *Yorpage* we obtained before this determination has been in good agreement.

4.9 The problem of young and very young families

In the previous Subsections we have pointed out that, in our analysis, some problems come out when discussing the properties of young families. There are several reasons.

- An obvious problem concerns the calibration we did to compare *Yorpage* with *Yarkage*. Our calibration entails a fixed offset of about $50My$, thus the minimum expected calibrated age is equal to this offset (for a nominal zero uncalibrated *Yorpage*). In this way we are –by definition– unable to fit ages below $50My$, and are presumably overestimating ages of families slightly older than this limit. In physical terms the reason is simple. The age at which the “eye” should appear is the sum of the time required to align the rotation axes, due to YORP, plus the time to change the semimajor axes, due to Yarkovsky effect, largely enough to be observed in the V–plot. Since YORP depends on the size

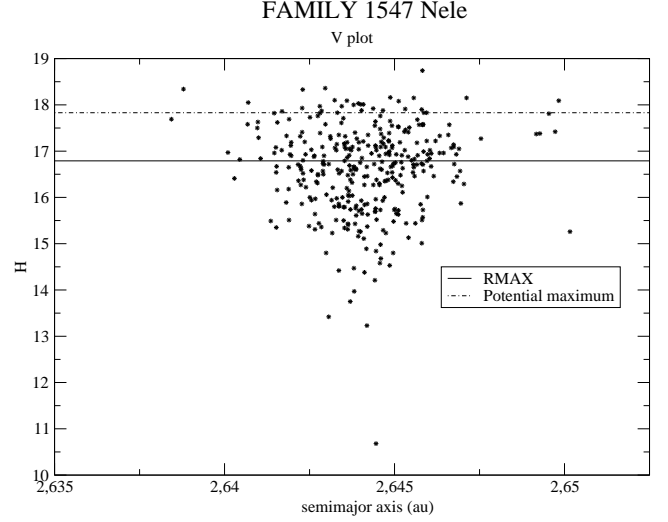


Figure 13. In the V plot of family 1547 we represent, with a horizontal line, the H value at which we find the significant maximum of $RMAX(H)$ which we adopted to estimate the *Yorpage*, and a possible alternative maximum (see text).

D as $1/D^2$ while Yarkovsky only on $1/D$, this additional term is negligible for old families, but not for young ones, the relevant sizes (or magnitudes H) to find the “eye” being smaller. Thus the presence of this fixed offset is, as for a first approximation, physically grounded. However, it is true that also the time required for a sufficient Yarkovsky driven mobility is shorter for the young families, the objects relevant for the detection of the evolution of the V–plot being smaller. In principle one might improve the fit with a size dependent offset. We decided not to do so for simplicity, also taking into account that, in our sample, the families for which this correction might be significant are very few. However it counts, as can be found also with the help of Figure 13. In the figure we represent the nominal $RMAX$, which corresponds, before the calibration, to a nominal age of about $7My$, in striking –but casual– agreement with the new age estimate, based on the convergence of secular angle, by Carruba et al. (2018). We might also, removing the control on the observational selection effects (see above) find another maximum, at about $mag = 17.8$, with a nominal age –before calibration– of about $2.5My$.

- Another problem concerns the values of H (or size) for which we should find significant footprints of the YORP/Yarkovsky evolution of the V–plot. They are, for families with ages of the order of a few *My*, clearly beyond the completeness limit; thus we are working on a subsample of the real members. This problem is serious, but we can expect that future observations may help to mitigate it. At present, the best age estimates for these families come out from dynamical computations, such as the “BIM” discussed by Carruba et al. (2018).

- Finally, some families are so young that no significant YORP/Yarkovsky evolution had the time to happen: they are the so-called “very young” families (Rosaev and Plávalová 2018). These families are presumably destined to remain, also in the future, unavailable for our analysis.

Table 6. For the un-Yarkaged families we give the number of significant maxima and the corresponding possible age range(s) (in *My*) suggested by the YORP analysis and calibrated to obtain the expected *Yarkage(s)*. We give also a synthetic estimate.

Corfam	Nmax	Expected Yarkage(s)(My)	synthetic guess
96 Aegle	3	195-244 404-525 777-1028	\approx 100-1000My
148 Gallia	1	91-119	\approx 100My
298 Baptistina	2	56-58 72-90	<100 My
410 Chloris	1	161-264	\approx 200My
490 Veritas	3	117-167 224-362 821-1447	\approx 200My or 1Gy
778 Theobalda	2	102-143 265-451	>100My
883 Matterania	2	69-86 104-163	\approx 100My
1118 Hanskya	2	146-190 2430-3589	\approx 150My or 3Gy
1222 Tina	2	68-75 96-116	\approx 100My
1298 Nocturna	2	172-263 431-1017	\approx 200 or 700My
1338 Duponta	3	59-65 72-92 97-147	\approx 100My
2782 Leonidas	3	105-125 171-217 558-756	\approx 150 or 600My
12739 1192DY7	3	59-68 66-94 89-173	\approx 100My
13314 1998RH71	1	134-176	\approx 150My
18466 1995SU37	2	66-78 87-121	\approx 100My
31811 1999NA41	2	81-107 120-182	\approx 100My

5 CONCLUSIONS AND OPEN PROBLEMS

In this paper we have finalized the method and the ideas presented in Paper I. The search of the YORP-eye has proven fruitful, and allows to obtain age estimates, in most cases in good agreement with the estimates obtained with the analysis based on Yarkovsky effect. Some families are unfit for the YORP analysis: typically old families, for which the “eye” should be located at small values of H where few bodies are present, or families for which there is a large gap in size among the one or few large fragments and the others; the algorithm is not being able to resolve the structure of the function $RMAX$ in the H region for which it is expected to be significant. In general, however, the method works well, and the frequent fair agreement between *Yorpage* and *Yarkage* supports the reliability of both estimates, and the assumptions behind them.

We have also introduced an estimate of the error of *Yorpage*, depending mainly on the dispersion of albedos. However, we have to remark again that the results suffer from other, partially unpredictable, uncertainties. Apart from the already discussed problem of calibration, which, however, the present direct comparison between *Yorpage* and *Yarkage* may help to resolve, we have other problems (interlopers, asymmetric structure of the family, different parameters working for different taxonomic types or even individual families, mixing of other dynamical effects, and so on). Thus we have to emphasize again that the outcomes from the present analysis provide only an indication, meaningful but not necessarily accurate enough, in need to be supported by other independent evidence.

Thus the values we obtain for the “un-Yarkaged families” are no more than a starting point for a thorough case-by-case analysis.

Finally we wish to remark, as already pointed out by Paolicchi et al. (2017) that a theoretical modelling, putting together original properties, Yarkovsky and YORP, dynamics and –last but not the least– collisions after the formation of the family, is urgently needed, to update and improve the pioneering approach by Vokrouhlický et al. (2006). This

project might also allow a better analysis concerning the young families.

A possible future analysis might be devoted also to the symmetry properties of the families, including also the analysis of the third (“Skewness”) and fourth momenta (“Kurtosis”) in the distributions of a , e , I . The Kurtosis analysis as a tool to understand the properties of asteroid families has been already introduced by Carruba and Nesvorný (2016), and has been devoted to the symmetry properties concerning the inclination I (or the velocity component v_w), obtaining useful indications about a few families, which have been studied in following papers. A 3–D analysis may be helpful to identify the combination of evolutionary processes, thus enabling to pass from a statistical study to the understanding of individual families, according to the ideas discussed also in the above quoted paper by Milani et al. (2018).

ACKNOWLEDGEMENTS

ZK acknowledges support from the Serbian Academy of Sciences and Arts via project F187, and by the Ministry of Education, Science and Technological Development of Serbia through the project 176011. PP acknowledges the funding by University of Pisa and INFN/TASP. We are grateful to the Referee V. Carruba for useful suggestions.

REFERENCES

- Bottke, W. F., Vokrouhlický, D., Rubincam, D. P., and Brož, M., 2002, Dynamical evolution of asteroids and meteoroids using the Yarkovsky effect. In *Asteroids III*, (Bottke, W.F. Jr., Cellino, A., Paolicchi, P., and Binzel, R.P., Eds.), Univ. of Arizona Press, Tucson, pp. 395-408
- Bottke, W.F., Vokrouhlický, D., Rubincam, D.P., and Nesvorný, D., 2006, The Yarkovsky and Yorp Effects: Implications for Asteroid Dynamics, *Ann. Rev. Earth Planet. Sci.* **34**, 157–191
- Bottke, W.F., Vokrouhlický, D., Walsh, K.J., Delbo, M., Michel, P., Lauretta, D. S., Campins, H., Connolly, H.C., Scheeres, D.J., and Chelsey, S.R., 2015, In search of the source of asteroid (101955) Bennu: Applications of the stochastic YORP model. *Icarus* **247**, 191-217

- Breiter, S., and Vokrouhlický, D., 2011, Yarkovsky-O'Keefe-Radzievskii-Paddack effect with anisotropic radiation, *MNRAS* **410**, 2807-2816
- Čapek, D. and Vokrouhlický, D., 2004, The YORP effect with finite thermal conductivity, *Icarus* **172**, 526-536
- Carruba, V., and D. Nesvorný, 2016, Constraints on the original ejection velocity fields of asteroid families, *MNRAS* **457**, 1332-1338
- Carruba, V., De Oliveira, E.R., Rodrigues, and I. Requena, 2018, The quest for young asteroid families: new families, new results, *MNRAS* **479**, 4815-4823
- Chesley, S. R., Ostro, S. J., Vokrouhlický, D., Čapek, D., Giorgini, J.D., Nolan, M.C., Margot, J.-L., Hine, A.A., Benner, L.A.M., and Chamberlin, A.B., 2003, Direct detection of the Yarkovsky effect via radar ranging to the near Earth asteroid 6489 Golevka, *Science*, **302**, 1739-1742
- Cotto-Figueroa, D., Statler, T.S., Richardson, D.C., and Tanga, P., 2015, Coupled Spin and Shape Evolution of Small Rubble-pile Asteroids: Self-limitation of the YORP Effect, *Astrophys. J.* **803**, Issue 1, article id. 25
- Dell'Oro A. and Cellino A., 2007, The random walk of Main Belt asteroids: orbital mobility by non-destructive collisions, *MNRAS* **380**, 399-416
- Farinella, P., Vokrouhlický, D., and Hartmann, W. K., 1998, Meteorite delivery via Yarkovsky orbital drift. *Icarus*, **132**, 378-387
- Farinella P., and Vokrouhlický D., 1999, Semimajor Axis Mobility of Asteroidal Fragments, *Science*, **283**, 1507-1510
- Hanuš, J., Ďurech, J., Brož, M., Warner, B. D., Pilcher, F., Stephens, R., Oey, J., Bernasconi, L., Casulli, S., Behrend, R., Polishook, D., Henych, T., Lehký, M., Yoshida, F., and Ito, T., 2011, A study of asteroid pole-latitude distribution based on an extended set of shape models derived by the lightcurve inversion method. *Astron. Astrophys.* **530**, id.A134
- Knežević, Z., Tsiganis, K., and Varvoglis, H., 2006, Age of the Veritas asteroid family from two independent estimates. *Pub. Astron. Obs. Belgrade* **80**, 161-166
- Kryszczyńska, A., La Spina, A., Paolicchi, P., Harris, A.W., Breiter, S., and Pravec, P., 2007, New findings on asteroid spin-vector distributions. *Icarus* **192**, 223-237
- La Spina, A., Paolicchi, P., Kryszczyńska, A., and Pravec, P., 2004, Retrograde spins of near-Earth asteroids from the Yarkovsky effect. *Nature* **428**, 400-401
- La Spina, A., Paolicchi, P., and Penco, U., 2005, Yarkovsky-evolved asteroid dynamical families: a correlation between their present properties and the impact geometry? American Astronomical Society, DPS meeting 37, 15.14; *Bull. American Astron. Soc.* **37**, 641
- Machuca, J.F. and V. Carruba, 2012, Secular dynamics and family identification among highly inclined asteroids in the Euprosyne region, *MNRAS* **420**, 1779-1798
- Micheli, M., and Paolicchi, P., 2008, YORP effect on real objects. I. Statistical properties. *Astron. Astrophys.* **490**, 387-391
- Milani, A., Cellino, A., Knežević, Z., Novaković, B., Spoto, F., and Paolicchi, P., 2014, Asteroid families classification: Exploiting very large datasets. *Icarus* **239**, 46-73
- Milani, A., Spoto, F., Knežević, Z., Novaković, B., and Tsirvoulis, G., 2016, Families classification including multiopposition asteroids. In: *Asteroids: New Observations, New Models*. Proceedings IAU Symposium 318 (Chesley, S., Farnocchia, D., Jedicke, R., and Morbidelli, A., Eds.), Cambridge University Press, Cambridge, pp. 28-45
- Milani, A., Knežević, Z., Spoto, F., Cellino, A., Novaković, B., and Tsirvoulis, G., 2017, On the ages of resonant, eroded and fossil asteroid families. *Icarus*, **288**, 240-264
- Milani, A., Knežević, Z., Spoto, F., and Paolicchi, P., 2018 Asteroid cratering families: recognition and collisional interpretation. *Astron. Astrophys.* submitted.
- Morbidelli, A., Nesvorný, D., Bottke W.F., Michel, P., Vokrouhlický, D. and P. Tanga, 2003, The shallow magnitude distribution of asteroid families, *Icarus* **162**, 328-336.
- Muñonen, K., Belskaya, I.N., Cellino, A., Delbò, M., Lévassieur-Regourd, A.-C., Penttilä, A., and Tedesco, E.F., 2010, A three-parameter magnitude phase function for asteroids. *Icarus* **209**, 542-555
- Nesvorný, D., and Vokrouhlický, D., 2008, Analytic theory for the YORP effect on obliquity. *Astron. J.*, **136**, 291-299
- Nesvorný, D., Brož, M., and Carruba, V., 2015, Identification and Dynamical Properties of Asteroid Families. In *Asteroids IV* (Michel, P., DeMeo, F.E, and Bottke, W.F., Eds.), University of Arizona, Tucson , pp. 297-322
- Novaković, B., 2010, Portrait of Theobalda as a young asteroid family, *MNRAS* **407**, 1477-1486
- Novaković, B., , Maurel, C., Tsirvoulis, G. and Knežević, Z., 2010, Dynamical portrait of the Hoffmeister asteroid family, *IAU General Assembly Meeting* **29**, id.2251337
- Paolicchi P., and Kryszczyńska, A., 2012, Spin vectors of asteroids: Updated statistical properties and open problems. *Planet. Space Sci.* **73**, 70-74
- Paolicchi P. and Knežević, Z., 2016, Footprints of the YORP effect in asteroid families. *Icarus* **274**, 314-326
- Paolicchi, P., Knežević, Z., Spoto, F., Milani, A., and Cellino, A., 2017, Asteroid "one-sided" families: Identifying footprints of YORP effect and estimating the age. *EPJP* **132**,7,id.307
- Pravec, P., Harris, A.W., and Michalowski, T., 2002, Asteroid Rotations. In: *Asteroids III* (Bottke, W.F. Jr., Cellino, A., Paolicchi, P., and Binzel, R.P., Eds.), Arizona Univ. Press, Tucson, pp. 113-122
- Pravec, P., Harris, A.W., Kušnirák, P., Galád, A., and Hornoch, K., 2012, Absolute magnitudes of asteroids and a revision of asteroid albedo estimates from WISE thermal observations. *Icarus* **221**, 365-387
- Rosaev, A. and E. Plávalová, 2018, On relative velocity in very young asteroid families. *Icarus* **304**, 135-142
- Rubincam D.P., 2000, Radiative Spin-up and Spin-down of Small Asteroids, *Icarus* **148**, 2-11
- Slivan, S.M., 2002, Spin vector alignment of Koronis family asteroids. *Nature* **419**, 49-51
- Spoto, F., Milani, A., and Knežević, Z., 2015, Asteroid family ages. *Icarus* **257**, 275-289
- Statler, T.S., 2009, Extreme sensitivity of the YORP effect to small-scale topography, *Icarus* **202**, 502-513
- Vereš, P., Jedicke, R., Fitzsimmons, A., Denneau, L., Granvik, M., Bolin, B., Chastel, S., Wainscoat, R.J., Burgett, W.S., Chambers, K.C., Flewelling, H., Kaiser, N., Magnier, E.A., Morgan, J.S., Price, P.A., Tonry, J.L., and Waters, C., 2015, Absolute magnitudes and slope parameters for 250,000 asteroids observed by Pan-STARRS PS1 - Preliminary results. *Icarus* **261**, 34-47
- Vokrouhlický, D., and Čapek, D., 2002, YORP-Induced Long-Term Evolution of the Spin State of Small Asteroids and Meteoroids: Rubincam's Approximation. *Icarus* **159**, 449-467
- Vokrouhlický, D., Nesvorný, D., and Bottke W. F., 2003, The vector alignments of asteroid spins by thermal torques. *Nature*, **425**, 147-151
- Vokrouhlický, D., Brož, M., Bottke, W.F., Nesvorný, D., and Morbidelli, A., 2006, Yarkovsky/YORP chronology of asteroid families. *Icarus* **182**, 118-142
- Vokrouhlický, D., Bottke, W. F., Chesley S.R., Scheeres D.J. and Statler T.S., 2015, The Yarkovsky and YORP effects. In *Asteroids IV* (Michel, P., DeMeo, F.E, and Bottke, W.F., Eds.), University of Arizona, Tucson, pp. 509-531

This paper has been typeset from a $\text{\TeX}/\text{\LaTeX}$ file prepared by the author.